

Biliverdine-Based Metalloradicals: Sterically Enhanced Noninnocence

Ingar Wasbotten and Abhik Ghosh*

Department of Chemistry, University of Tromsø, N-9037 Tromsø, Norway

Received November 27, 2005

This is a first density functional theory survey of transition-metal biliverdines (Blv), where we have chosen to focus on key Mn, Fe, Co, and Cu complexes. According to the calculations, the complexes are invariably noninnocent, featuring $\text{Blv}^{\bullet 2-}$ ligand radicals. In this, biliverdine complexes resemble metallochorroles, but the parallels are only approximate. Briefly, metallobiliverdines exhibit a much greater tendency to adopt noninnocent electronic structures than analogous metallochorroles. The $\text{O}\cdots\text{O}$ nonbonded contacts in biliverdines apparently preclude the formation of short metal–N bonds that, in turn, could stabilize high-valent metal ions. Thus, while most copper chorroles (Cor) exhibit diamagnetic Cu^{III} ground states, copper biliverdines are clearly $\text{Cu}^{\text{II}}\text{Blv}^{\bullet 2-}$ species. In the same spirit, while chloroiron chorroles are best described as $\text{Fe}^{\text{III}}(\text{S} = 3/2)\text{Cor}^{\bullet 2-}$, the analogous biliverdine derivative seems best described as $\text{Fe}^{\text{III}}(\text{S} = 5/2)\text{Blv}^{\bullet 2-}$, i.e., featuring a high-spin Fe^{III} center with long (>2.0 Å) Fe–N bond distances. Overall, the results highlight the important role that steric effects may play in modulating the electronic structures and the potentially noninnocent nature of transition-metal complexes.

Introduction

The recent blossoming of transition-metal chorrole¹ chemistry has provided an instructive chemical context against which we can appreciate the electronic structures' high-valent heme protein intermediates. Thus, just as formally iron(V) compound **I** intermediates are best described as $\text{Fe}^{\text{IV}}\text{OPor}^{\bullet -}$,² so are formally iron(IV) chloride chorroles better described

as $\text{Fe}^{\text{III}}(\text{S} = 3/2)\text{Cor}^{\bullet 2-}$ (Por = porphyrin; Cor = chorrole). Like chorroles, the formally trianionic biliverdines³ are also recognized as noninnocent ligands; however, except for one important density functional theory (DFT)⁴ study on *redox-inactive* metal complexes, metallobiliverdines have remained largely unexplored by theoretical methods. Biliverdine is an important metabolite that arises from the oxidative breakdown of heme by the action of the enzyme heme oxygenase. The helical structures of natural biliverdine and its synthetic analogues (which have different substitution patterns and will simply be referred to as biliverdines from this point onward)⁵ endow them with a fascinating coordination chemistry as well as novel chiroptical properties. Here we present a first

* To whom correspondence should be addressed. E-mail: abhik@chem.uit.no.

- (1) Relevant papers on chorroles: (a) Ghosh, A.; Wondimagegn, T.; Parusel, A. B. *J. Am. Chem. Soc.* **2000**, *122*, 5100–5104. (b) Cai, S.; Walker, F. A.; Licocchia, S. *Inorg. Chem.* **2000**, *39*, 3466–3478. (c) Steene, E.; Wondimagegn, T.; Ghosh, A. *J. Phys. Chem. B* **2001**, *105*, 11406–11413. Addition/Correction: *J. Phys. Chem. B* **2002**, *106*, 5312–5312. (d) Zakhariyeva, O.; Schunemann, V.; Gerdan, M.; Licocchia, S.; Cai, S.; Walker, F. A.; Trautwein, A. X. *J. Am. Chem. Soc.* **2002**, *124*, 6636–6648. (e) Steene, E.; Dey, A.; Ghosh, A. *J. Am. Chem. Soc.* **2003**, *125*, 16300–16309. (f) Isocorrole: van Oort, B.; Tangen, E.; Ghosh, A. *Eur. J. Inorg. Chem.* **2004**, 2442–2445. (g) Simkhovich, L.; Gross, Z. *Inorg. Chem.* **2004**, *43*, 6136–6138 and references cited therein. (h) Nardis, S.; Paolesse, R.; Licocchia, S.; Fronczek, F. R.; Vicente, M. G. H.; Shokhireva, T. K.; Cai, S.; Walker, F. A. *Inorg. Chem.* **2005**, *44*, 7030–7046. (i) Norcorrole: Ghosh, A.; Wasbotten, I. H.; Davis, W.; Swarts, J. C. *Eur. J. Inorg. Chem.* **2005**, 4479–4485. (j) Harischandra, D. N.; Zhang, R.; Newcomb, M. *J. Am. Chem. Soc.* **2005**, *127*, 13776–13777.
- (2) (a) Groves, J. T. In *Cytochrome P450: Structure, Mechanism, and Biochemistry*, 3rd ed.; Ortiz de Montellano, P. R., Ed.; Kluwer/Plenum: New York, 2005; pp 1–43. (b) Shaik, S.; de Visser, S. P. In *Cytochrome P450: Structure, Mechanism, and Biochemistry*, 3rd ed.; Ortiz de Montellano, P. R., Ed.; Kluwer/Plenum: New York, 2005; pp 45–85. (c) Ghosh, A.; Steene, E. *J. Biol. Inorg. Chem.* **2001**, *6*, 739–752. (d) Wasbotten, I. H.; Conradie, J.; Ghosh, A. *J. Inorg. Biochem.* **2006**, *100*, 502–506.

- (3) Relevant papers on transition-metal biliverdines: (a) Review: Mizutani, T.; Yagi, S. *J. Porphyrins Phthalocyanines* **2004**, *8*, 226–237. (b) Iron: Balch, A. L.; Latos-Grazynski, L.; Noll, B. C.; Olmstead, M. M.; Safari, N. *J. Am. Chem. Soc.* **1993**, *115*, 9056–9061. (c) Copper: Balch, A. L.; Mazzanti, M.; Noll, B. C.; Olmstead, M. M. *J. Am. Chem. Soc.* **1993**, *115*, 12206–12207. (d) Nickel and palladium: Lord, P. A.; Olmstead, M. M.; Balch, A. L. *Inorg. Chem.* **2000**, *39*, 1128–1134. (e) Palladium: Lord, P. A.; Noll, B. C.; Olmstead, M. M.; Balch, A. L. *J. Am. Chem. Soc.* **2001**, *123*, 10554–10559. (f) Manganese: Spasojevic, I.; Batinic-Haberle, I.; Stevens, R. D.; Hambright, P.; Thorpe, A. N.; Grodkowski, J.; Neta, P.; Fridovich, I. *Inorg. Chem.* **2001**, *40*, 726–739. (g) Iron: Nguyen, K. T.; Rath, S. P.; Latos-Grazynski, L.; Olmstead, M. M.; Balch, A. L. *J. Am. Chem. Soc.* **2004**, *126*, 6210–6211.
- (4) Sztrenberg, L.; Latos-Grazynski, L.; Wojaczynski, J. *ChemPhysChem* **2003**, *4*, 691–698.
- (5) Goessuer, A. In *The Porphyrin Handbook*; Kadish, K. M., Smith, K. M., Guillard, R., Eds.; Academic: San Diego, 2003; Vol. 13, Chapter 84, pp 237–274.

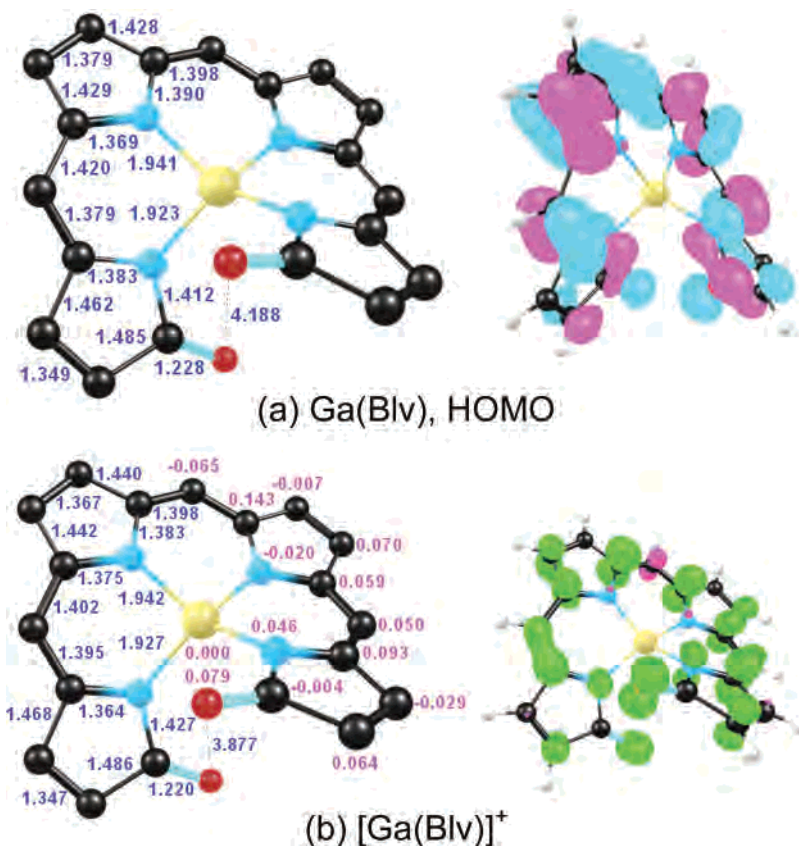


Figure 1. (a) Ga(Blv): key distances (Å) in optimized geometry and HOMO. (b) [Ga(Blv)]⁺: distances (Å, blue), spin populations (magenta), and spin-density plot (majority spin in green; minority spin in magenta).

DFT survey of first-row transition-metal biliverdines (also known as 1,19-bilindiones), M(Blv): while, not surprisingly, several results parallel those obtained for corroles, there are intriguing differences as well. Gratifyingly, the results afford some unexpected insights into the factors influencing ligand noninnocence in high-valent transition-metal complexes.

Methods

Throughout this study, we have used spin-unrestricted DFT calculations with full geometry optimizations, the VWN local functional, PW91 gradient corrections for both exchange and correlation,^{6–8} all-electron triple- ζ plus polarization Slater-type basis sets, a fine mesh for numerical integrations of matrix elements, and tight criteria for geometry optimizations, all as implemented in the ADF 2004 program system.⁹ These methods have been documented to provide a generally good description of high-valent metalloporphyrins and related compounds.^{10,11} In addition, for certain molecules, we have evaluated noniterative post-self-consistent-field (SCF) energies for different electronic states (which were initially

optimized with the PW91 functional) for a variety of exchange-correlation functionals, including PW91,^{10–12} BLYP,^{12,13} RPBE,¹⁴ revPBE,¹⁵ OLYP,^{16,17} mPBE,¹⁸ OPBE,^{19,20} B3LYP(VWN5),^{21–23} and O3LYP(VWN5).^{22,24}

Results

Gallium Biliverdine. The gallium complex Ga(Blv) serves as a redox-inactive reference against which we can analyze the electronic structures of open-shell transition-metal biliverdines. The porphyrin four-orbital model,²⁵ which also applies to corroles,^{1a} does not apply to biliverdines; however, the highest occupied molecular orbital (HOMO, which has A

(6) Perdew, J. P. In *Electronic Structure of Solids*; Ziesche, P., Eschrig, H., Eds.; Akademie: Berlin, 1991; p 11.
 (7) Perdew, J. P.; Chevary, J. A.; Vosko, S. H.; Jackson, K. A.; Pederson, M. R.; Singh, D. J.; Fiolhais, C. *Phys. Rev. B* **1992**, *46*, 6671–6687.
 (8) Perdew, J. P.; Chevary, J. A.; Vosko, S. H.; Jackson, K. A.; Pederson, M. R.; Singh, D. J.; Fiolhais, C. *Phys. Rev. B* **1993**, *48*, 4978–4978.
 (9) For a description of the ADF program, see: Velde, G. T.; Bickelhaupt, F. M.; Baerends, E. J.; Guerra, C. F.; Van Gisbergen, S. J. A.; Snijders, J. G.; Ziegler, T. J. *J. Comput. Chem.* **2001**, *22*, 931–967.
 (10) Ghosh, A.; Steene, E. *J. Biol. Inorg. Chem.* **2001**, *5*, 739–752.
 (11) Ghosh, A. *Acc. Chem. Res.* **2005**, *38*, 943–954.

(12) Becke, A. D. *Phys. Rev. A* **1988**, *38*, 3098–3100.
 (13) Lee, C.; Yang, W.; Parr, R. G. *Phys. Rev. B* **1988**, *37*, 785–789.
 (14) Hammer, B.; Hansen, L. B.; Norskov, J. K. *Phys. Rev. B* **1999**, *59*, 7413–7421.
 (15) Zhang, Y.; Yang, W. *Phys. Rev. Lett.* **1998**, *80*, 890.
 (16) Handy, N. C.; Cohen, A. J. *Mol. Phys.* **2001**, *99*, 403–412.
 (17) Lee, C.; Yang, W.; Parr, R. G. *Phys. Rev. B* **1988**, *37*, 785–789.
 (18) Adamo, C.; Barone, V. *J. Chem. Phys.* **2002**, *116*, 5933–5940.
 (19) Perdew, J. P.; Burke, K.; Ernzerhof, M. *Phys. Rev. Lett.* **1996**, *77*, 3865–3868.
 (20) Perdew, J. P.; Burke, K.; Ernzerhof, M. *Phys. Rev. Lett.* **1997**, *78*, 1396–1396.
 (21) Stephens, P. J.; Devlin, F. J.; Chabalowski, C. F.; Frisch, M. J. *J. Phys. Chem.* **1994**, *98*, 11623–11627.
 (22) Watson, M. A.; Handy, N. C.; Cohen, A. J. *J. Chem. Phys.* **2003**, *119*, 6475–6481.
 (23) Hertwig, R. H.; Koch, W. *Chem. Phys. Lett.* **1997**, *268*, 345–351.
 (24) Cohen, A. J.; Handy, N. C. *Mol. Phys.* **2001**, *99*, 607–615.
 (25) For recent work on the four-orbital model, see: Vangberg, T.; Lie, R.; Ghosh, A. *J. Am. Chem. Soc.* **2002**, *124*, 8122–8130 and references cited therein.

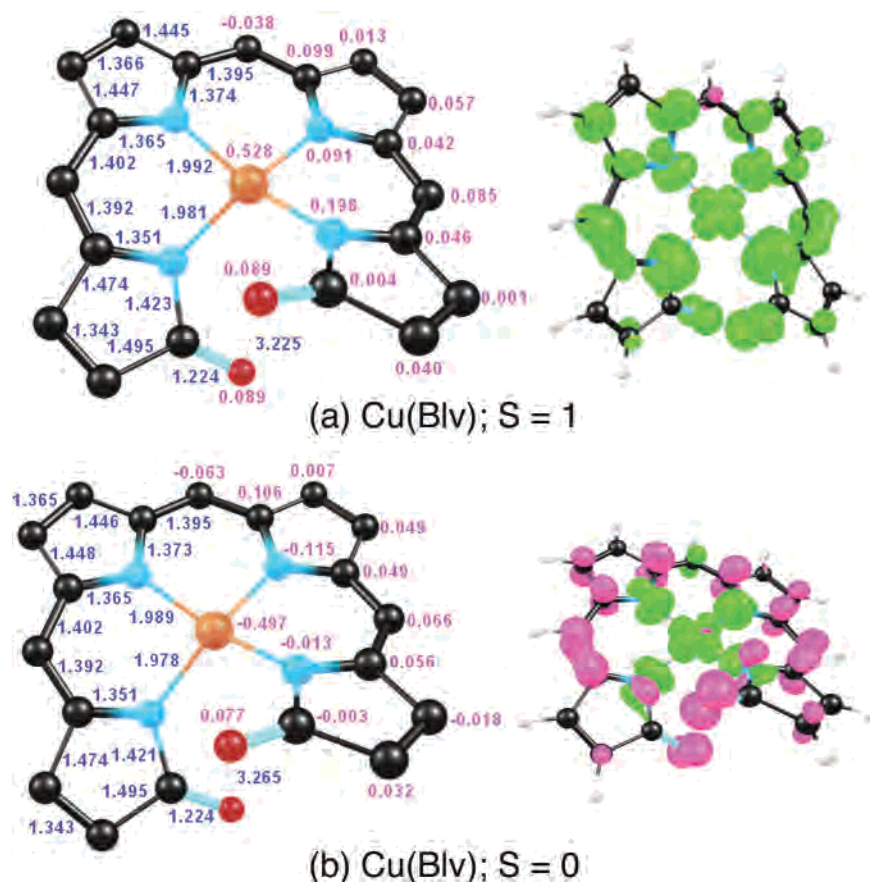


Figure 2. Cu(Blv): distances (Å, blue), spin populations (magenta), and spin-density plot (majority spin in green; minority spin in magenta).

symmetry) and HOMO-1 (which has B symmetry) crudely resemble the porphyrin a_{1u} and a_{2u} HOMOs, respectively. Thus, for Ga(Blv) (C_2 ; Figure 1a,b), the two lowest adiabatic ionization potentials are 6.7 and 7.6 eV, which correspond to the lowest 2A and 2B states of $[\text{Ga}(\text{Blv})]^+$, respectively. The spin-density profile of $[\text{Ga}(\text{Blv})]^+$ exhibits a curious blob of *minority* spin density at the unique meso carbon, as well as *majority* spin blobs at the two symmetry-related meso carbons. As pointed out in an earlier DFT study,⁴ this spin distribution nicely captures the observed ^1H NMR chemical shift pattern of $\text{Fe}(\text{OEBlv})\text{Cl}$ ($\text{OEBlv} = \beta$ -octaethylbiliverdine).^{3g}

We should note that the (lowest) calculated ionization potential of Ga(Blv) is almost identical to that of Ga(Cor) (6.7 eV).^{1a} Yet, we will see that transition-metal biliverdines are distinctly more noninnocent, i.e., have a greater degree of ligand radical character, than analogous metallochorroles. Toward the end of the paper, we will make an attempt to explain this enigmatic finding.

Copper Biliverdine. For Cu(Blv) (C_2 ; Figure 2a,b), near-degenerate ferro- and antiferromagnetically coupled $\text{Cu}^{\text{II}}\text{Blv}^{2-}$ states, with Cu–N distances of about 1.98 Å, are obtained as the lowest-energy states, while a closed-shell Cu^{III} state with short Cu–N distances is about 0.5 eV higher in energy. These findings are qualitatively consistent with experimental electron paramagnetic resonance measurements.^{3c} In contrast, copper corroles generally exhibit diamagnetic Cu^{III} ground states with short Cu–N distances, albeit with thermally

accessible $\text{Cu}^{\text{II}}\text{Cor}^{2-}$ excited states.^{1e,26} Comparisons with certain additional macrocyclic complexes are instructive. Thus, for isocorrole,^{1f} which has a slightly smaller N_4 core than corrole, DFT clearly favors a Cu^{III} ground state, although this result remains to be experimentally confirmed. In the same vein, a Cu^{III} ground state is favored by a substantial margin of energy for corrolazine,²⁷ which has a considerably tighter N_4 core than corrole.

Iron (and Manganese) Biliverdine Chloride. For $\text{Fe}(\text{Blv})\text{Cl}$ (Figure 3a–c), the PW91 optimized $S = 1$ and 2 states are near-degenerate, while the $S = 3$ state is 0.51 eV higher in energy. The spin populations and spin-density profiles shown in Figure 3 indicate that the $S = 1$ and 2 states may be described as antiferro- and ferromagnetically coupled $\text{Fe}^{\text{III}}(S = 3/2)\text{Blv}^{2-}$, while the $S = 3$ state is ferromagnetically coupled $\text{Fe}^{\text{III}}(S = 5/2)\text{Blv}^{2-}$. Interestingly, the Fe–N distances in the calculated $S = 1$ and 2 states (all

(26) (a) Halvorsen, I.; Wondimagegn, T.; Ghosh, A. *J. Am. Chem. Soc.* **2002**, *124*, 8104–8116. (b) Ou, Z.; Shao, J.; Zhao, H.; Ohkubo, K.; Wasbotten, I. H.; Fukuzumi, S.; Ghosh, A.; Kadish, K. M. *J. Porphyrins Phthalocyanines* **2004**, *8*, 1236–1247. (c) Brückner, C.; Brinas, R. P.; Bauer, J. A. K. *Inorg. Chem.* **2003**, *42*, 4495–4497. (d) Luobeznova, I.; Simkhovich, L.; Goldberg, I.; Gross, Z. *Eur. J. Inorg. Chem.* **2004**, *8*, 1724–1732.

(27) (a) Ramdhanie, B.; Stern, C. L.; Goldberg, D. P. *J. Am. Chem. Soc.* **2001**, *123*, 9447–9448. (b) Mandimutsira, B. S.; Ramdhanie, B.; Todd, R. C.; Wang, H.; Zareba, A. A.; Czernuszewicz, R. S.; Goldberg, D. P. *J. Am. Chem. Soc.* **2002**, *124*, 15170–15171 and references cited therein. (c) Tangen, E.; Ghosh, A. *J. Am. Chem. Soc.* **2002**, *124*, 8117–8121. (d) Fox, J. P.; Ramdhanie, B.; Zareba, A. A.; Czernuszewicz, R. S.; Goldberg, D. P. *Inorg. Chem.* **2004**, *43*, 6600–6608.

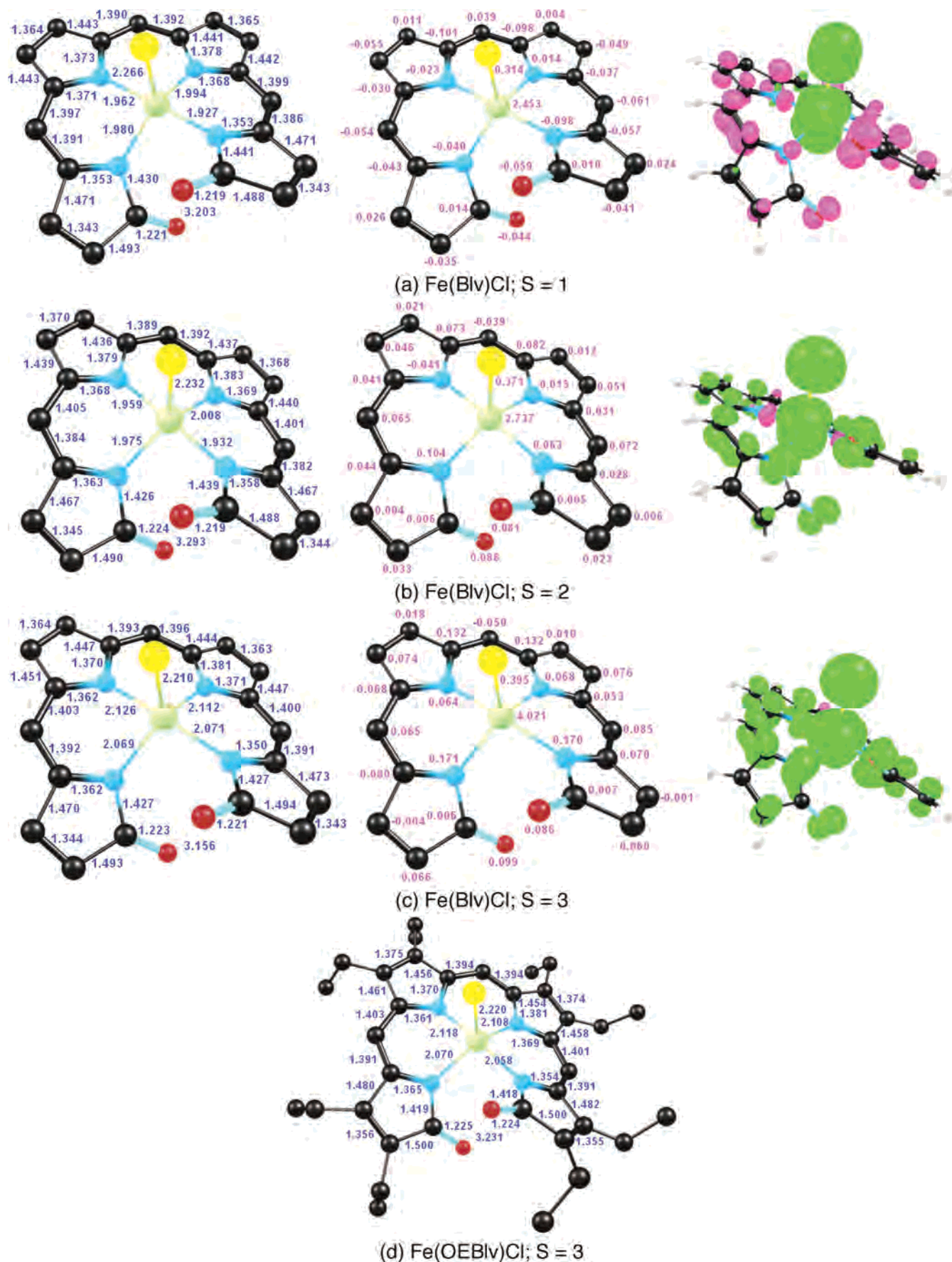


Figure 3. Fe(Blv)Cl: distances (Å, blue), spin populations (magenta), and spin-density plot (majority spin in green; minority spin in magenta).

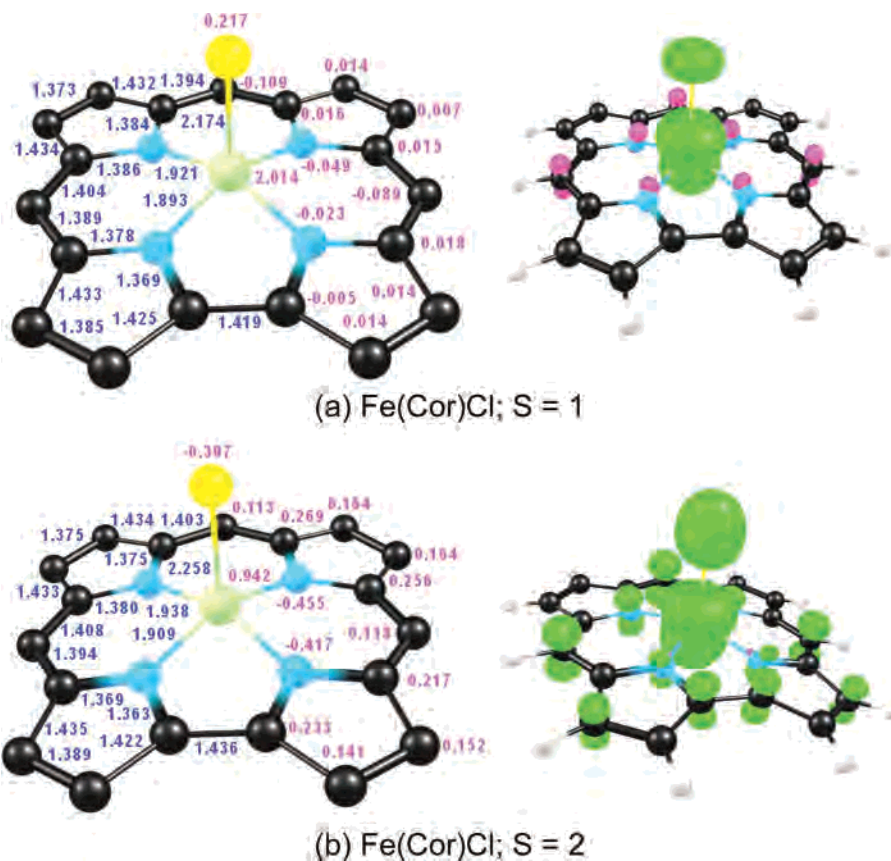


Figure 4. $\text{Fe}(\text{Cor})\text{Cl}$: distances (Å, blue), spin populations (magenta), and spin-density plot (majority spin in green; minority spin in magenta).

Table 1. Calculated DFT Energetics (eV) of Different Low-Lying Spin States of Chloroiron Corroles and Biliverdines

compound	S	PW91	single-point energies at PW91 geometries							
			BLYP	RPBE	revPBE	OLYP	mPBE	OPBE	B3LYP	O3LYP
$\text{Fe}(\text{Cor})\text{Cl}$	1	0.00	0.00	0.00	0.00	0.00	0.00	0.00	0.00	0.00
	2	0.53	0.49	0.45	0.46	0.36	0.49	0.39	0.32	0.29
$\text{Fe}(\text{Ph}_3\text{Me}_8\text{Cor})\text{Cl}$	1	0.00	0.00	0.00	0.00	0.00	0.00	0.00	0.00	0.00
	2	0.42	0.38	0.34	0.35	0.25	0.38	0.28	0.26	0.21
$\text{Fe}(\text{Blv})\text{Cl}$	1	0.00	0.00	0.00	0.00	0.00	0.00	0.00	0.00	0.00
	2	0.00	0.03	-0.01	-0.01	-0.05	-0.01	-0.08	0.18	0.05
	3	0.54	0.42	0.24	0.29	-0.07	0.40	-0.03	-0.11	-0.29

<2.0 Å) are significantly shorter than those observed experimentally for $\text{Fe}(\text{OEBIv})\text{Cl}$.^{3g} To see if this discrepancy resulted from our neglect of the ethyl groups, we also optimized the $S = 1-3$ states of $\text{Fe}(\text{OEBIv})\text{Cl}$. The results clearly showed that the long, experimentally observed $\text{Fe}-\text{N}$ distances were best reproduced in the $S = 3$ optimized structure (Figure 3d), i.e., only with a high-spin Fe^{III} center. We already knew from several calibration studies that many commonly used functionals, including PW91, exhibit a significant energetic bias in favor of lower-spin states.²⁸ Consequently, as shown in Table 1, we calculated single-point post-SCF energies for the $S = 1-3$ states of $\text{Fe}(\text{Blv})\text{Cl}$ for a variety of exchange-correlation functionals. Interestingly, the hybrid functionals B3LYP and O3LYP do favor the $S = 3$ state as the ground state. Thus, in spite of

the higher calculated PW91 energies for the $S = 3$ states, the calculated and experimental geometries,^{3g} in a nice synergy, strongly suggest a high-spin $\text{Fe}^{\text{III}}\text{OEBIv}^{2-}$ description for $\text{Fe}(\text{OEBIv})\text{Cl}$.

This electronic description for $\text{Fe}(\text{Blv})\text{Cl}$ contrasts significantly with that for chloroiron corroles (Figure 4). Most chloroiron corrole complexes, such as those based on *meso*-triarylcorroles and β -octafluoro-*meso*-triarylcorroles, exhibit $S = 1$ ground states, reflecting an antiferromagnetically coupled $\text{Fe}^{\text{III}}(S = 3/2)\text{Cor}^{2-}$ electronic configuration.¹ However, Walker and co-workers have recently presented NMR evidence (chemical shift patterns and magnetic susceptibilities) that the modestly saddled complex $\text{Fe}(\text{OMTPC})\text{Cl}$ (OMTPC = β -octamethyl-*meso*-triphenylcorrole) exhibits an $S = 2$ ground state, reflecting a ferromagnetically coupled $\text{Fe}^{\text{III}}(S = 3/2)\text{Cor}^{2-}$ electronic configuration.^{1h} However, note from Table 1 that all of the functionals examined fail to indicate an $S = 2$ ground state for $\text{Fe}(\text{OMTPC})\text{Cl}$, presumably reflecting the imperfect nature of the currently available exchange-correlation functionals. While we have not inves-

(28) (a) Ghosh, A.; Vangberg, T.; Gonzalez, E.; Taylor, P. *J. Porphyrins Phthalocyanines* **2001**, *5*, 345–356. (b) Ghosh, A.; Persson, B. J.; Taylor, P. R. *J. Biol. Inorg. Chem.* **2003**, *8*, 507–511. (c) Ghosh, A.; Taylor, P. R. *Curr. Opin. Chem. Biol.* **2003**, *7*, 113–124. (d) Ghosh, A.; Taylor, P. R. *J. Chem. Theory Comput.* **2005**, *1*, 597–600.

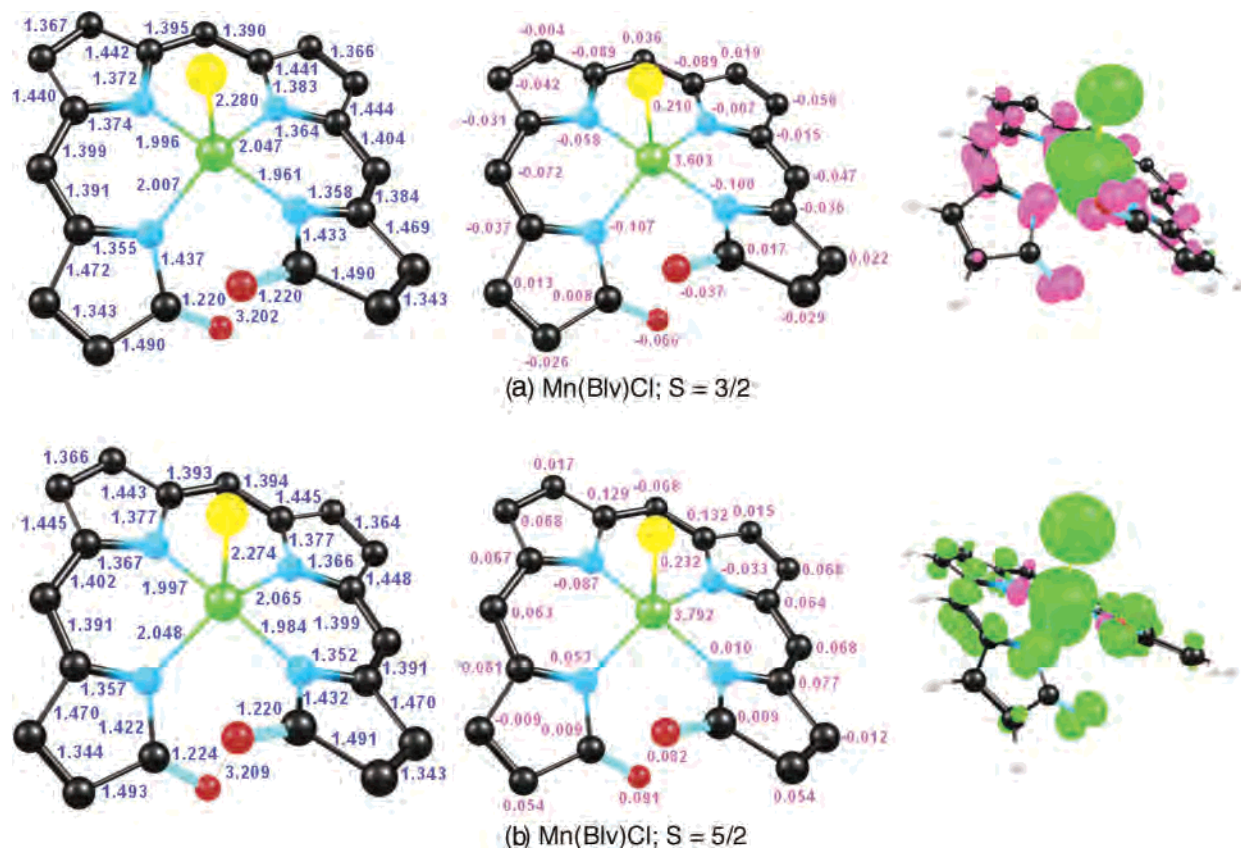


Figure 5. Mn(Blv)Cl: distances (Å, blue), spin populations (magenta), and spin-density plot (majority spin in green; minority spin in magenta).

tigated the detailed reason behind the antiferro- vs ferro-magnetic coupling in different corrole derivatives (our focus here being on biliverdines), the $S = 3/2$ Fe^{III} nature of the Fe center seems relatively well established.¹ In contrast, we have argued that iron chloride biliverdines feature $S = 5/2$ Fe^{III} centers, which highlights a key difference between corroles and biliverdines.

Our results on Mn(Blv)Cl largely parallel those on Fe(Blv)Cl. The spin populations and spin-density plots shown in Figure 5 show that both the $S = 3/2$ and $5/2$ states of Mn(Blv)Cl are clearly describable as $\text{Mn}^{\text{III}}(S = 2)\text{Blv}^{2-}$. Both states were also found to be equienergetic. A significant distinction between Mn(Blv)Cl and Fe(Blv)Cl lies in the metal–N bond distances, reflecting the importance of half-occupancy of the Fe $d_{x^2-y^2}$ orbital whose lobes point more or less directly at the biliverdine N atoms. Note, however, that the PW91 optimized geometries Fe(Cor)Cl and Mn(Cor)Cl exhibit rather similar metal–N distances because the Fe is only intermediate-spin in the corrole complex.^{1c}

Metal–Phenyl Complexes. By analogy with the corrole derivatives, we have assumed $S = 1$, $3/2$, and $1/2$ for the Fe–, Mn–, and Co–phenyl biliverdine complexes (Figure 6a–c), respectively. However, here too there are significant differences from corrole.^{1d,f,i} While the Fe–phenyl and Mn–phenyl corrole derivatives feature relatively innocent corrole rings (i.e., with little spin density),^{1d,f} the metal centers in Fe(Blv)Ph and Mn(Blv)Ph harbor only about 75–80% of the total molecular spin; the rest is largely delocalized onto the noninnocent biliverdine ligand. In the same vein, only

about a quarter of the spin of Co(Blv)Ph resides on the Co, clearly indicating a $\text{Co}^{\text{III}}\text{PhBlv}^{2-}$ electronic configuration.

Discussion

What accounts for the ubiquitous, if not universal, noninnocence of transition-metal-complexed biliverdine ligands? This is actually a rather intriguing issue, given that Ga(Blv) and Ga(Cor) exhibit nearly identical ionization potentials, implying that high-valent metallobiliverdines should be no more noninnocent than analogous metallocorroles. Careful examination of our results indicates that the enhanced noninnocence of biliverdines stems from the sterics of their own architecture. The $\text{O}\cdots\text{O}$ nonbonded contacts preclude short metal–N distances favored by high-valent middle- and late-transition-metal ions, something that corroles and corrolazines, being cyclic, readily accommodate.²⁹

An interesting clue in this connection comes from the fact that Ga(Blv) features a significantly longer $\text{O}\cdots\text{O}$ distance than the various transition-metal complexes examined. An examination of the MOs of Ga(Blv) confirms that Ga, as a main-group element, favors an sp^3 -type tetrahedral coordination sphere, unlike the transition-metal centers examined here. In general, the $\text{O}\cdots\text{O}$ separation appears to reflect a compromise between $\text{O}\cdots\text{O}$ sterics, on the one hand, and

(29) Interestingly, note that the $\text{O}\cdots\text{O}$ distance is significantly longer in Ga(Blv) than in the transition-metal complexes. An examination of the MOs of this compound confirms the expectation that Ga, as a main-group element, favors an sp^3 -type tetrahedral coordination sphere, unlike the transition-metal centers examined here.

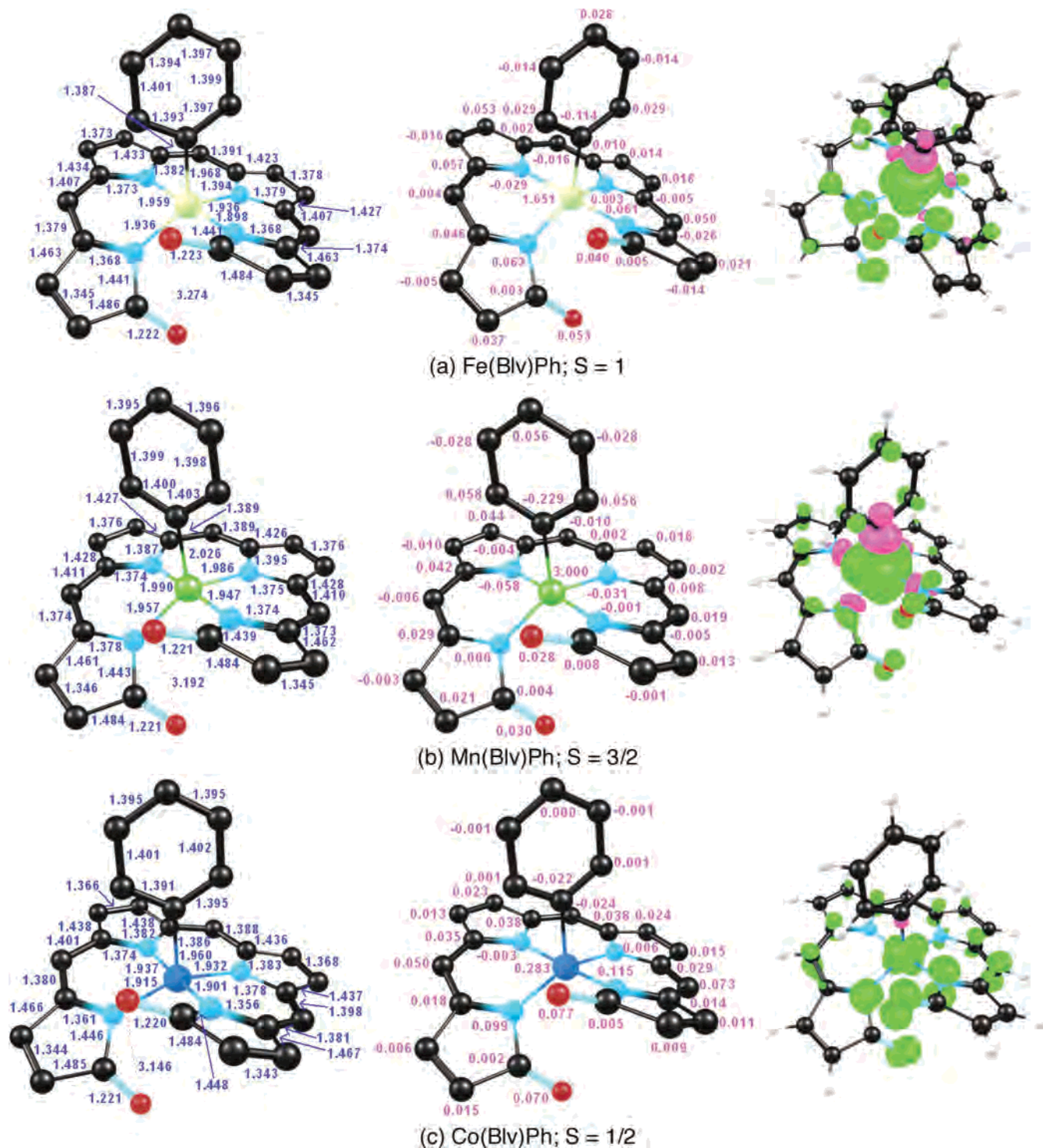


Figure 6. Metal–phenyl complexes: distances (Å, blue), spin populations (magenta), and spin-density plot (majority spin in green; minority spin in magenta).

metal d orbital interactions favoring a flatter N_4 coordination sphere, on the other hand.

Obviously, steric modulation of metal–ligand orbital interactions is by no means unique to biliverdins, and the present results need to be viewed against a broader context. Thus, oxidized metalloporphyrins also exhibit a variety of geometry-dependent metal–porphyrin spin couplings, as a function of the ruffling, saddling, and doming distortions.³⁰ A plethora of geometry-dependent metal–radical interactions

are also seen in nonheme enzymes, of which galactose oxidase is a notable example.³¹ Last, as an example of a conscious use of ligand sterics for spin-state engineering,

(30) (a) Ghosh, A.; Gonzalez, E.; Vangberg, T. *J. Phys. Chem. B* **1999**, *103*, 1363–1367. (b) Ghosh, A.; Halvorsen, I.; Nilsen, H. J.; Steene, E.; Wondimagegn, T.; Lie, R.; van Caemelbecke, E.; Guo, N.; Ou, Z. P.; Kadish, K. M. *J. Phys. Chem. B* **2001**, *105*, 8120–8124. (c) Shao, J. L.; Steene, E.; Hoffman, B. M.; Ghosh, A. *Eur. J. Inorg. Chem.* **2005**, *8*, 1609–1615. (d) Cheng, R. J.; Wang, Y. K.; Chen, P. Y.; Han, Y. P.; Chang, C. C. *Chem. Commun.* **2005**, 1312–1314.

we may recall the bioinspired $\text{Fe}^{\text{III}}\text{Fe}^{\text{IV}}(\mu\text{-O})_2$ intermediates, where changing the terminal supporting ligand from tpa [tris-(2-pyridylmethyl)amine] to 6-me₃-tpa results in dramatic changes in the electronic and geometric structures of the “diamond” cores.³² In closing, we hope that the insights obtained here will contribute to new findings on metal–radical chemistry and spin-state engineering.

Conclusions

We have presented here a first DFT survey of transition-metal biliverdine derivatives. The results indicate the strong tendency of biliverdines to exist as $\text{Blv}^{\bullet 2-}$ radicals. Thus, noninnocence increases along the series porphyrin \rightarrow corrole \rightarrow biliverdine. Some striking examples of the biliverdine radical character are as follows.

While copper corroles are generally diamagnetic Cu^{III} species with low-lying $\text{Cu}^{\text{II}}\text{Cor}^{\bullet 2-}$ excited states, copper biliverdine is clearly $\text{Cu}^{\text{II}}\text{Blv}^{\bullet 2-}$, the Cu^{III} state being too high in energy to be a contender for the ground state.

Both $\text{Fe}(\text{Cor})\text{Cl}$ and $\text{Fe}(\text{Blv})\text{Cl}$ feature noninnocent tetrapyrrole ligands, but while the Fe center in $\text{Fe}(\text{Cor})\text{Cl}$ is best described as $S = 3/2$ Fe^{III} , the Fe in $\text{Fe}(\text{Blv})\text{Cl}$ seems to be high-spin Fe^{III} , indicating that the biliverdine ligand exerts a weaker ligand field compared with corrole.

(31) Whittaker, J. W. *Chem. Rev.* **2003**, *103*, 2347–2363.

A comparison of $\text{Fe}(\text{Cor})\text{Ph}$ and $\text{Fe}(\text{Blv})\text{Ph}$, as well as analogous Mn derivatives, also confirms the increased noninnocent tendencies of biliverdine, compared with corrole.

Given that both corrole and biliverdine are trianionic ligands, what accounts for the much greater noninnocence of the latter? The fact that $\text{Ga}(\text{Cor})$ and $\text{Ga}(\text{Blv})$ exhibit nearly identical ionization potentials suggests that electronic factors do not account for the difference in noninnocent character between Cor and Blv ligands in transition-metal complexes. Instead, it appears that $\text{O}\cdots\text{O}$ steric repulsion plays the key role in this matter: in other words, this steric constraint prevents metallobiliverdines from adopting short metal–ligand distances that would be conducive to the stabilization of high-valent metal oxidation states. Thus, compared with corroles, the noninnocence of biliverdines seems to be sterically enhanced.

Acknowledgment. This work was supported by grants from the Research Council of Norway.

Supporting Information Available: Optimized Cartesian coordinates. This material is available free of charge via the Internet at <http://pubs.acs.org>.

IC052037W

(32) Que, L.; Tolman, W. B. *Angew. Chem., Int. Ed.* **2002**, *41*, 1114–1137.